

Demonstrating the Scientific Benefits of Adaptive Optics through Imaging & Spectroscopy of Stars at the Center of the Milky Way Galaxy

A. M. Ghez & S. Gezari

University of California Los Angeles, Department of Physics and Astronomy, Los Angeles, CA 90095-1562

Abstract.

Adaptive Optics on large ground-based telescopes presents the opportunity to do new types of astronomical science. In this contribution, we focus on one example of science that has been recently enabled with this advance. Adaptive Optics has, for the first time, allowed studies of the individual stars located 0."1 to 0."5 (4 to 20 light days) away from the putative supermassive ($2.6 \times 10^6 M_{\odot}$) black hole at the center of our Galaxy. These stars are important as probes both of the dark matter distribution and of the central black hole's effects on the local environment.

1. Introduction

The construction of large ground-based optical and infrared telescopes is driven by the desire to obtain both higher sensitivity and higher angular resolution astronomical measurements. With each increase in telescope diameter the goal of increased sensitivity has been achieved. In contrast, the angular resolution of large telescopes ($D > 1$ m), using traditional imaging, is limited not by the diffraction limit, but rather by turbulence in the atmosphere. At $2.2 \mu m$ on Mauna Kea this is typically 0."5, a factor of 10 times worse than the theoretical limit of the Keck telescope.

This angular resolution handicap has led to the development of a number of techniques for producing diffraction-limited observations. These techniques cover a wide range of complexity and performance. The "simplest" method, and thus generally the first to be implemented, is the passive method of speckle imaging. This technique requires many short exposures ($t_{exp} \sim 100msec$), which are post-processed to produce high resolution images. Although this technique has produced a number of exciting results (e.g., Ghez et al. 1993, 1998; Koresko 1998; Koresko et al. 1999; Gibbard et al. 1999) it has limited dynamic range ($\Delta K_{lim} \sim 4$) and is limited to producing images. The future of high spatial resolution work is in Adaptive Optics (AO), where real-time atmospheric corrections are made, allowing both high dynamic range images and spectroscopic observations of the object of interest to be taken at high spatial resolution.

An excellent example of the power of AO is in studies of stars at the center of our Galaxy. Figure 1 shows that these stars are only detectable with the use of a high angular resolution imaging technique. Located within approximately 0."5

(\sim a light-month) of the center of our Galaxy, these stars are powerful probes of that environment. Prior to the advent of AO, speckle imaging was used to measure their motion on the plane of the sky (proper motions). This work provided strong evidence for a central supermassive blackhole ($2.6 \times 10^6 M_{\odot}$, coincident with the unusual radio source Sgr A*, through the discovery of stars at small galactocentric distances with high velocities that fall off as $1/r^2$ (Genzel 1997, 2000; Ghez et al. 1998, 2000). Adaptive Optics offers a much more powerful means for studying these stars. In particular, it is now possible to obtain spectra of these stars. Such observations, in principle, would provide the first measurements of their radial velocities. The stellar radial velocity measurements combined with the proper motion measures would yield the full, 3-dimensional velocities. The added information from radial velocities would strongly constrain the possible orbital solutions. Figure 2 shows the range of orbital solutions for S0-2, one of the stars in the Sgr A*(IR) cluster, based on the proper motion data alone. On the right are the predicted radial velocities in June 2000 for all of the acceptable orbits, showing that a successful radial velocity measurement would greatly constrain the solutions for the high proper motion stars with a single measurement. With near diffraction-limited resolution spectroscopy, it would also be possible to characterize the spectral type of the stars in the central arcsecond (see Figure 3). The orbits and spectral types would provide insight into several questions regarding the environment surround our Galaxy's central black hole. In particular, it would allow us to determine (1) from the spectral types, whether or not star formation occurs in this region and (2) from the orbits, whether or not there is an additional source of dark matter surrounding the central black hole, perhaps in the form of an entourage of stellar remnants.

1.1. Observations

Simultaneous K band (2.0 - 2.4 μm) spectra and images of stars in the Sgr A* (IR) Cluster were obtained using NIRSPEC (McLean et al. 1998) behind the AO system (Wizinowich et al. 2000) on the W.M. Keck II 10 meter telescope during three nights of observations on 2000 June 20-22 (UT). Near diffraction limited spatial resolution was achieved with adaptive optics using a R = 13.2 mag natural guide star, located 30" away from Sgr A*. The observed AO corrected point spread function (PSF) was composed of a near diffraction limited core on top of a seeing halo. Figure 4 shows the FWHM of the PSF's core and fraction of energy it contained based on measurements of IRS 16C in the $t_{int} = 10$ sec images of the central 4.4" x 4.4" taken with the slit viewing camera (SCAM), plate scale = 0.0171"/pixel, during the spectroscopic observations with SPEC. The AO performance during the nights of June 20 and 21, when the PSF contained a median of ~ 30 % of the total energy in a 0."09 core, were somewhat better than on June 22, when the PSF contained a median of ~ 25 % of the total energy in a 0."1 core.

Spectra were obtained with a 3.96" x 0.036" slit in low resolution mode, resulting in a moderate spectral resolution of $\lambda/\Delta\lambda \sim 2000$. Figure 5 shows the position of the slit on the SgrA* (IR) Cluster for each night of observations. On June 20 the slit was centered on S0-16¹ (K = 15.3 mag), a new and variable source

¹named following conversion outlined in Ghez et al. 1998

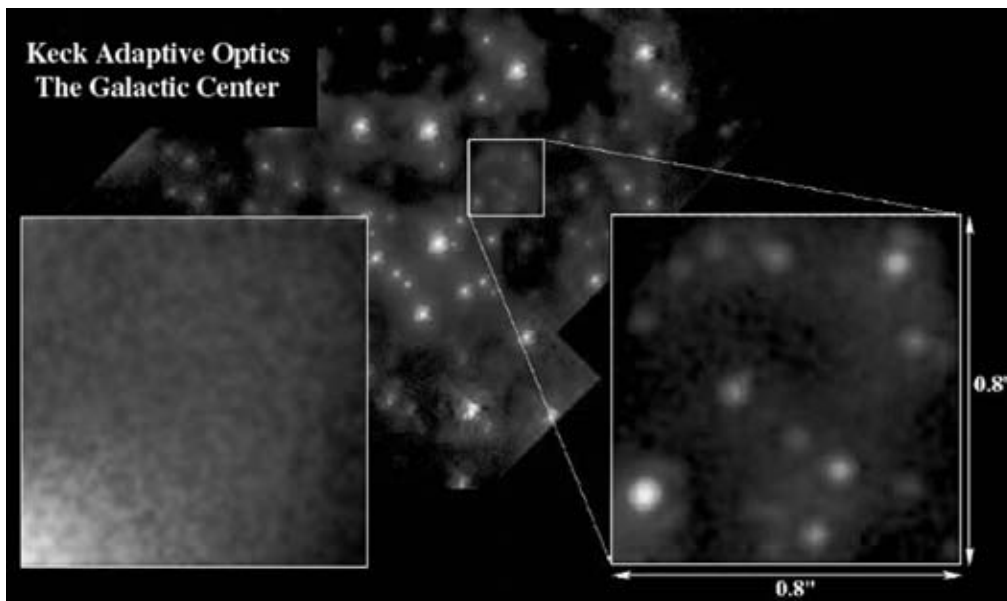


Figure 1. An image of the center of the Milky Way Galaxy. The insets show the central $0.8'' \times 0.8''$ with AO off (left) and AO on (right). In this region, stars are detectable only with the use of high angular resolution imaging. (This image was produced in collaboration with O. Lai and P. Wizinowich of Keck Observatory).

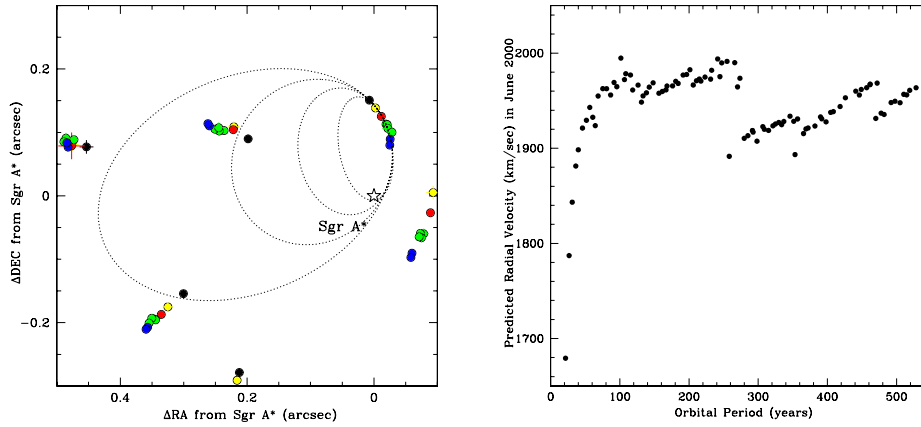


Figure 2. On the left are the proper motion measurements (1995 - 1999) and possible orbital solutions for S0-2, the star with the largest acceleration, 0.3 cm/sec^2 , in the plane of the sky. Each of the acceptable orbits has a predictable June 2000 radial velocity, which is plotted on the right. The values are both large and distinct. Therefore a successful radial velocity measurement would easily distinguish between the current possible solutions, demonstrating the spectroscopic differences between the two possibilities.

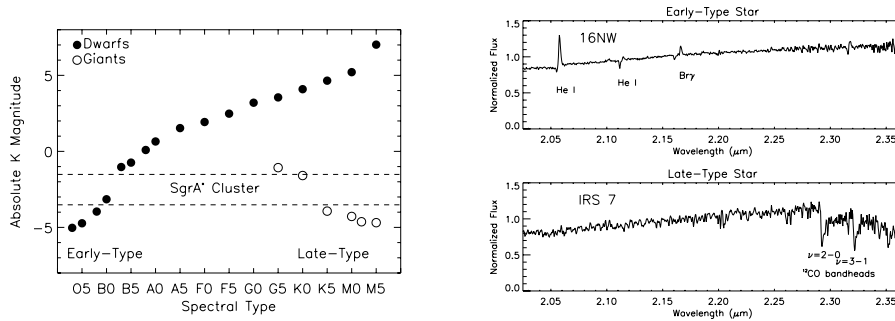


Figure 3. (Left) Possible spectral types for the Sgr A* (IR) Cluster sources given their range of absolute K magnitudes in relation to standard dwarf and giant stars. Based on this they are expected to either be early type dwarfs or late-type giants (Right) Examples of early type (IRS 16NW) and late type stars (IRS 7) in the bright Galactic Center stellar population.

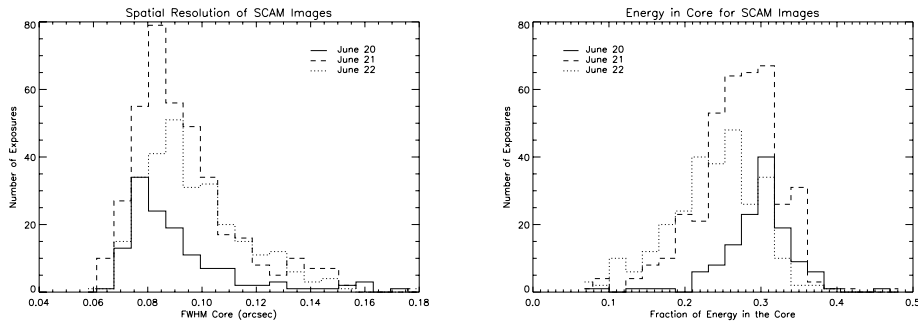


Figure 4. Histograms of the FWHM (left), and fraction of energy in the core (right), of the AO corrected PSF in the $t_{int} = 10$ sec SCAM images taken during each night of observations.

detected by Ghez et al. (2001, in preparation) coincident with the position of Sgr A*, and S0-17 ($K = 16.0$ mag) and on June 21 and 22 the slit was centered on the Sgr A* Cluster stars S0-1 ($K = 14.9$ mag), S0-2 ($K = 14.1$ mag), and S0-18 ($K = 15.1$ mag). The slit was aligned so that the bright star IRS 16NW ($K = 10.1$ mag) was in the slit for each $t_{int} = 300$ sec exposure, in order for the exposures to be easily shifted and added together in post processing of the data. A total of 45, 100, 80 minute of integration time were obtained on June 20, 21, and 22, respectively.

1.2. Results

Figure 6 shows the calibrated 2D spectra for each night, and figure 7 shows the spatial profile of the Sgr A* Cluster stars in the final 2D spectra averaged from 2.20 to 2.28 μm , in average counts per pixel. A 1D spectrum for each star was extracted from the final 2D spectrum from each night by carrying out a weighted average across 15 pixels ($\sim 0.''2$) in the spatial direction, centered on the peak of the star, by weights set by the PSF profile of IRS 16NW as measured in the 2D spectrum. 1D spectra of the sky (including gas and unresolved stars) in the regions between IRS 16NW and S0-16 on June 20, and the region between IRS 16NW and S0-2 on June 21 and June 22, were also extracted by averaging across the same width in the spatial direction. The signal-to-noise ratios of the spectra extracted from the June 22 spectrum were a factor of two worse than from those obtained on June 21 and therefore were not used in the remaining analysis. Figure 8 shows the 1D spectra extracted for the Sgr A* Cluster stars observed on June 20 and June 21, compared to the sky spectrum extracted each night.

The absolute K magnitudes of the observed stars, assuming a distance of 8 kpc (Reid 1993) and 3 mag of extinction to the Galactic Center, can be fit by stars of two different spectral types: 1) late O - early B dwarfs or 2) early K giants (see Figure 3). The K-band spectra of these two populations of stars are distinctive because of the deep CO absorption bandheads in the late-type giants, and the He I lines and H I Br γ line in the early-type stars. Therefore each star's spectrum is examined for these lines, whose positions are labeled with tick marks in Figure

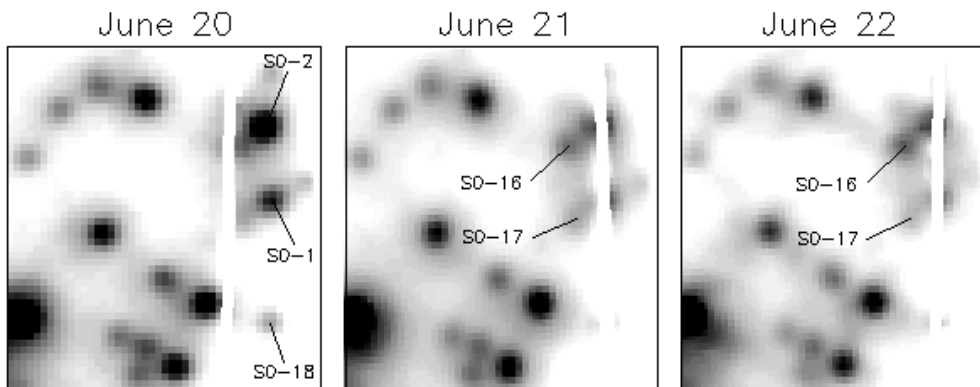


Figure 5. Co-added SCAM images of the Sgr A* Cluster, clipped down to the central $0.77'' \times 0.86''$, to show the position of the slit during the spectroscopic observations on June 20, June 21, and June 22.

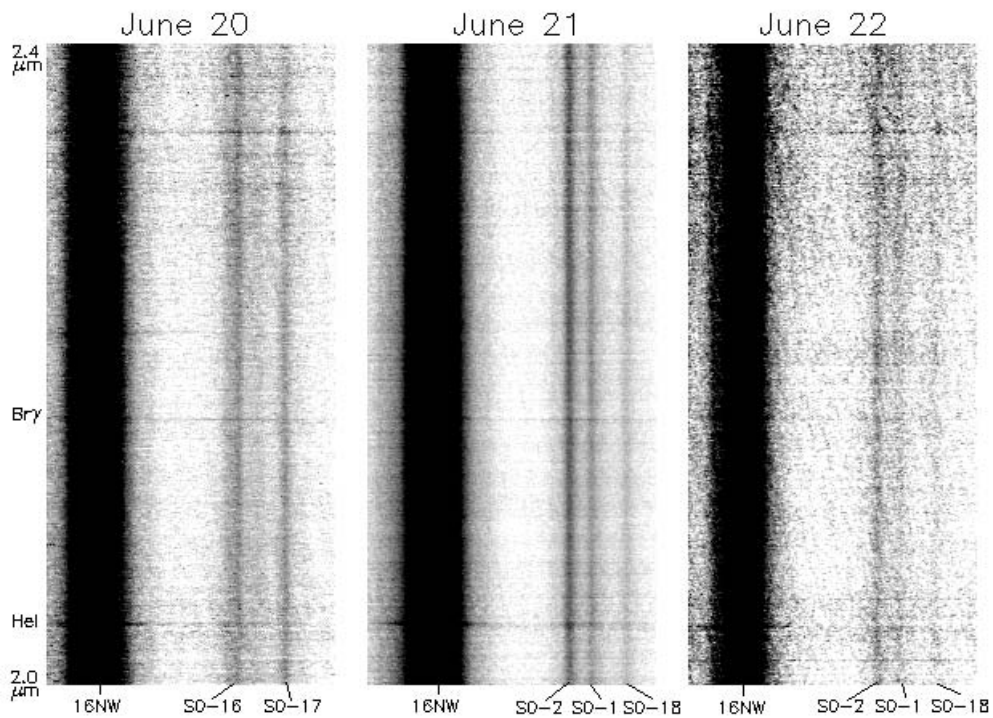


Figure 6. Final 2D K-band spectra for each night of observations.

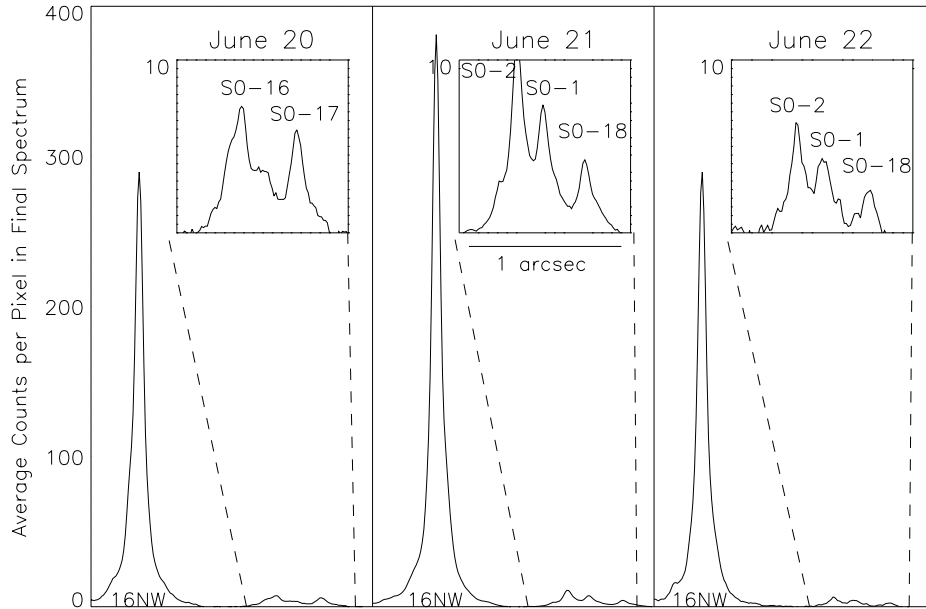


Figure 7. Spatial profile of the final 2D spectra averaged from 2.20 to 2.28 μm in counts per pixel.

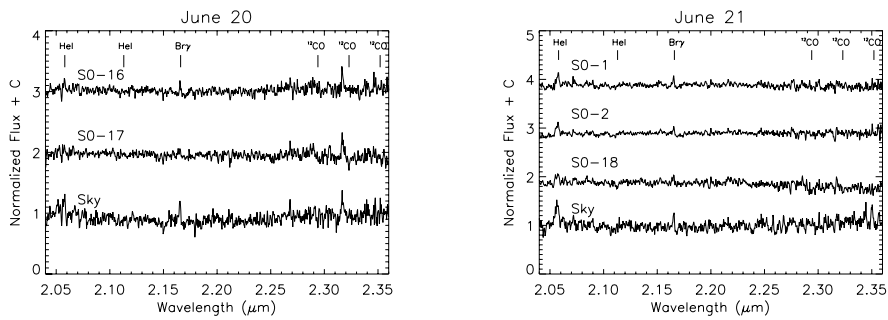


Figure 8. K-band spectra of the Sgr A* (IR) Cluster sources observed June 20 and June 21 in comparison to the sky. The spectra are normalized to their flux at 2.20 μm , and shifted by increments of 1.

8. The feature at $2.316 \mu m$, seen in emission on June 20 and in absorption on June 21, is an atmosphere line that was not properly removed in the telluric correction.

Late-type spectral features: CO bandhead absorption CO bandhead absorption is easily identified in late-type stars because of its distinctive line shape and bandhead spacing. In order to identify CO bandheads in the low signal-to-noise Sgr A* Cluster spectra, the extracted spectrum of each source was cross correlated with the spectrum of the K0-III spectral standard, HD 203638. Figure 9a shows the correlation of the wavelength range from 2.24 to $2.36 \mu m$, which includes the ^{12}CO (2,0), ^{12}CO (3,1), ^{13}CO (2,0), and ^{12}CO (4,2) absorption bandheads for each of the Sgr A* Cluster stars observed. The K0-III standard spectrum and the Sgr A* Cluster spectra in this wavelength range were normalized and the slope of the continuum removed before cross correlating them. S0-1, S0-2, and S0-16 clearly show no evidence of positive correlation with the K0-III spectrum, whereas S0-17 and S0-18 have tentative correlation peaks. Although the low correlation values are relatively low, ~ 0.4 , and the implied velocity shift is similar for the two sources, ~ 70 km/s, we follow through the implications of these tentative detections. Figure 9b shows their normalized spectra shifted in the wavelength direction to the velocity of the correlation peak. The negative correlation peak can be attributed to the strong atmosphere line that was poorly corrected for in the June 20 spectrum. The dotted line in figure 9a shows the cross correlation function after the atmosphere line at $2.316 \mu m$ was replaced by a section of the spectrum immediately to the left of it. It is seen that the deep negative correlation peak mostly vanishes after the rough removal of the atmosphere line, shown in figure 9b. The velocity shift of the correlation peak for S0-17 and S0-18 was used to measure CO bandhead absorption at the appropriate wavelengths, and the other sources lacking a correlation with the K0-III spectrum (S0-1, S0-2, and S0-16) were also measured at these velocity shifts to determine upper limits on absorption strengths due to systematic errors.

Absorption strengths for the CO bandheads, $1 - F_{CO}/F_{cont}$, were measured using a bandwidth of $\Delta\lambda = 0.0055 \mu m$ for the CO absorption and continuum fluxes, where the continuum was measured to the left of the first CO bandhead at $2.29 \mu m$, in order to match the methods used in the Kleinmann and Hall (1986) $2.0 - 2.5 \mu m$ spectral atlas of late-type standard stars. The slope in the continuum of the spectra from 2.00 to $2.29 \mu m$ was fit by a line and removed before measuring absorption strengths. The statistical error in the absorption strength measurements was estimated by the jackknife resampling method (Babu and Feigelson, 1996). In this method, the 1 sigma error is determined from the dispersion of measurements from random half sets of data from the original value. Figure 10 shows the CO bandhead absorption strengths with 1 sigma error bars measured for each source at the CO bandhead wavelengths identified by the location of the peak of the cross correlation of S0-17 and S0-18 with the K0-III standard. Absorption strengths for standard stars ranging from G8-III to K5-III from Kleinmann and Hall (1986) are plotted with dashed lines, and the absorption strengths measured for the observed K0-III standard, HD 203638, are plotted with diamonds. S0-17 and S0-18 both have ^{12}CO (2,0), ^{12}CO (3,1), and ^{13}CO (2,0) absorption strengths consistent with a K0 giant (within 3σ) for both the Kleinmann and Hall (1986) K0-III standard, and the K0-III standard

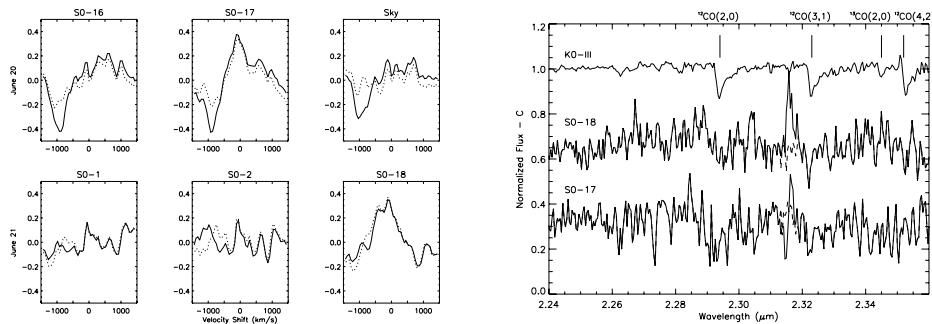


Figure 9. a) Cross correlation function of SgrA* Cluster source spectra and sky with the K0-III standard spectrum from 2.24 to 2.36 μm , with the dotted line showing the cross correlation function after the atmosphere line at 2.316 μm was removed. b) Normalized spectra of those Sgr A* Cluster stars with correlation peaks with the K0-III standard, shifted to the velocity of the correlation peak, and shifted down by an offset of 0.3 and 0.7 for S0-17 and S0-18 respectively. Dotted line shows the spectra with the atmosphere line replaced by the spectrum immediately left to it.

observed in this analysis. These absorption strength measurements support the tentative correlation peaks with the K0-III giant spectrum, suggesting that these stars are in fact late-type giants. The other sources, S0-1, S0-2, and S0-16 show absorption strengths consistent with no detection (within 3σ) for all three CO band heads measured, consistent with their lack of correlation with a K0-III spectrum; this strongly suggests that these stars lack CO bandhead absorption, and are therefore early-type stars.

1.3. Early-type spectral features: He I and $Br\gamma$

In addition to a lack of CO bandhead absorption, early-type main sequence stars can be identified by their He I lines at 2.058 μm and 2.113 μm , and H I $Br\gamma$ line at 2.166 μm . Figure 11 shows the line equivalent widths for these features as a function of spectral type for late O - early B main sequence stars from Hanson et al. (1996). The H I $Br\gamma$ absorption line is the strongest feature in this range of spectral types, and is the most sensitive line to stellar temperature. Its absorption equivalent width monotonically increases from 1 Angstrom for an O5 star up to 7 Angstrom for a B5 star. The He I lines at 2.058 μm and 2.113 μm , on the other hand, have weak absorption equivalent widths ($< \sim 1$ Angstrom), and their strengths do not have an obvious dependence on temperature. In the spectral class range we are interested in for the Sgr A* Cluster, the $Br\gamma$ line appears to be the most useful diagnostic for spectral classification. Unfortunately, the Sgr A* (IR) Cluster spectra are heavily contaminated at 2.166 μm by $Br\gamma$ emission from ionized gas in the region. This is demonstrated in the 2D spectrum from June 20 and June 21 (Figure 6), where $Br\gamma$ is seen in emission across the spectrum. Due to the strong background gas emission, $Br\gamma$ absorption intrinsic to the Sgr A* Cluster stars very hard to detect. Although we cannot detect

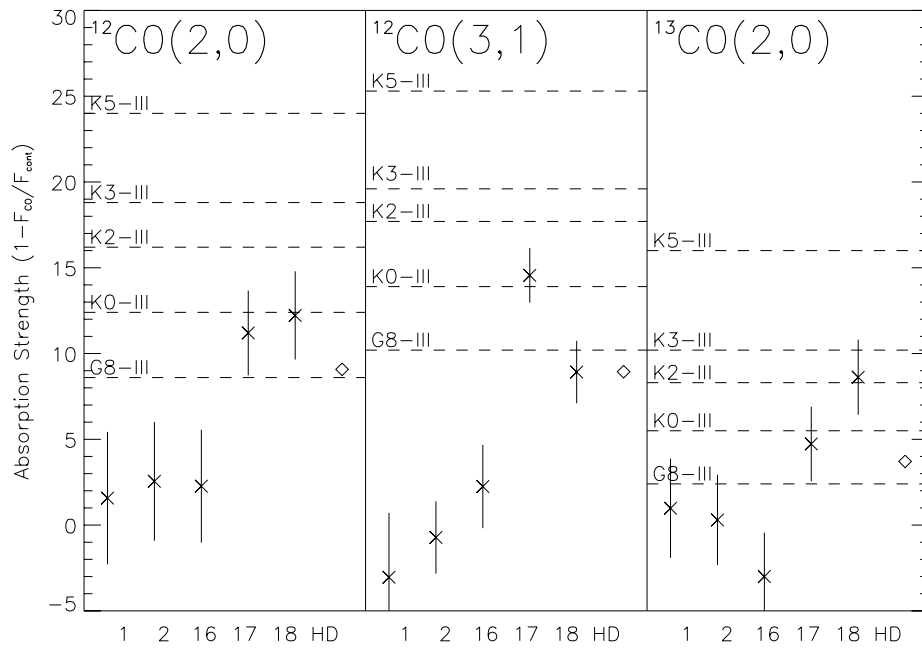


Figure 10. CO Bandhead absorption measurements (plotted as percentage) with 1 sigma error bars for the Sgr A* Cluster stars in comparison to absorption strengths measured for spectral standard stars from Kleinmann and Hall (1986) shown with dashed lines. Diamonds show measurements for K0-III standard observed, HD 203638.

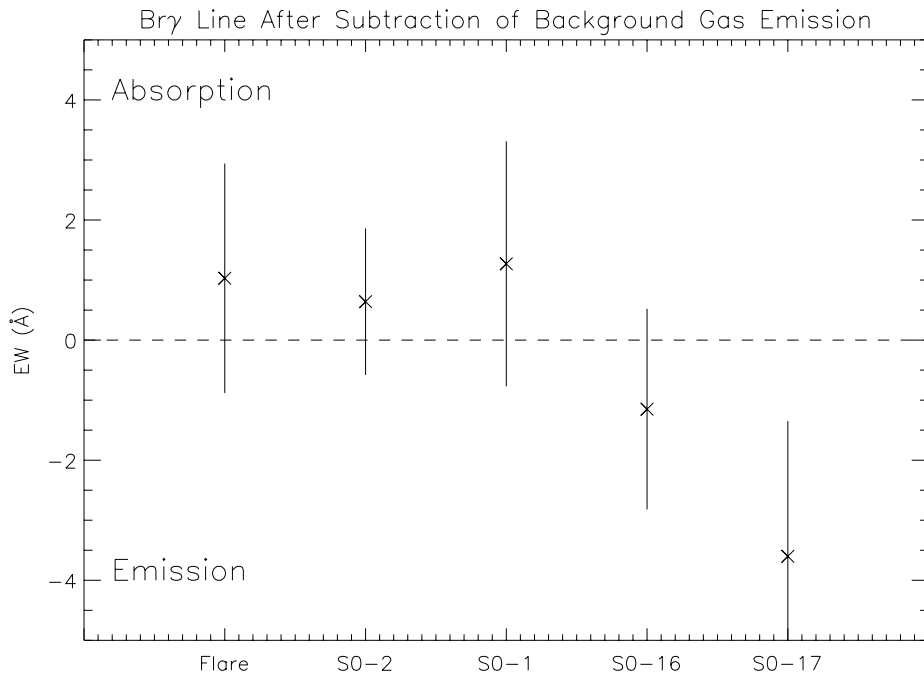


Figure 11. $\text{Br}\gamma$ line equivalent widths with 1σ error bars for the Sgr A* Cluster stars after the line flux from the background gas emission has been subtracted out.

the absorption lines in the Sgr A* Cluster stars directly, we can put limits on the equivalent widths of their absorption lines by subtracting out the integrated flux of background $\text{Br}\gamma$ emission from the stellar spectra, and then measuring the equivalent width of their $\text{Br}\gamma$ line. The equivalent widths were measured at $2.166\ \mu\text{m}$, using a bandwidth of $\Delta\lambda = 0.02\ \mu\text{m}$ in order to allow for doppler shifts of the lines from the rest wavelength of up to $\pm 1500\ \text{km/s}$. Figure 11 shows the $\text{Br}\gamma$ line equivalent widths measured for the Sgr A* Cluster stars after the line emission from the sky has been subtracted out.

Within 2σ , S0-17 and S0-18 do not demonstrate $\text{Br}\gamma$ absorption in their spectra, consistent with their classification as early K giants. Their equivalent widths are also consistent with $\text{Br}\gamma$ emission, which can be attributed to residual $\text{Br}\gamma$ emission from incomplete removal of background contamination from the stellar spectra. The stars classified as early-type, S0-1, S0-2, and S0-16 do demonstrate $\text{Br}\gamma$ absorption, and their equivalent widths are within the range measured for late O - early B main sequence stars (within 2σ). However, given the large errors in their equivalent widths, $1\sigma \sim 2\text{\AA}$, and the uncertainties in subtraction of the background contamination, it is not practical to use these absorption strengths to classify the stars within this spectral range. In addition, difficulties in measuring lines in this region of the spectrum arise from uncertainties in the removal of the $\text{Br}\gamma$ absorption line in the telluric standard spectrum. Hanson et

al. (1996) emphasize that this is their largest source of systematic error in their Br γ line equivalent widths.

The He I 2.058 μm line is also contaminated by emission from background ionized He I gas. However, even without problems of background emission, both He I lines at 2.058 μm and 2.113 μm have absorption strengths that are intrinsically too low to be detected in the Sgr A* Cluster spectra, which have EW errors up to 3 Angstroms. The very low signal-to-noise ratios of the Sgr A* Cluster spectra, and the strong contamination by background gas emission makes identification of early-type spectral features intrinsic to the stars in the spectra not feasible at this time. However, the indirect measurement of Br γ absorption in S0-1, S0-2, and S0-16 does support the argument that they are in fact early-type main sequence stars.

1.4. Discussion and Conclusions

Spectral Types The lack of CO bandhead absorption in the moderate resolution spectra of three Sgr A* Cluster stars (S0-1, S0-2, and S0-16), is direct evidence that these stars are early-type, and with their absolute K magnitudes, that they are late O - early B main sequence stars, which implies ages less than 20 Myr. The existence of young stars in the immediate vicinity of a central supermassive black hole is surprising, considering the extreme conditions expected to inhibit star formation in such an environment. Morris (1993) discusses how the strong magnetic fields (\sim mG), large turbulent velocities ($v \sim 10$ km/s), high temperatures, and the large tidal forces induced by the central black hole in the Galactic Center would only enable star formation in gas clouds of very high densities. Gas near the Galactic Center would have to be compressed to densities 5 orders of magnitude higher than their current densities in order to avoid tidal disruption and be able to gravitationally collapse to form stars. Such a violent compression of the gas clouds could be triggered externally by cloud collisions, stellar winds, and supernova shocks in the Galactic Center. Although this seems problematic, the early-type stars in the Sgr A* Cluster star suggests that star formation is indeed possible in this tidally extreme environment.

Radial Velocities The radial velocities measured from the doppler shifts of the CO bandheads in S0-16 and S0-17 can be added to their proper motion velocities to get their true three dimensional velocities. If we assume that these stars are in bound orbits around the central supermassive black hole, then we can determine upper limits on their current distance from the black hole from $r < 2GM_{bh}/v_{3D}^2$. The upper distance limits of these stars from Sgr A* are 0.1 pc for S0-17, and 0.3 pc for S0-18. The velocities of these stars cannot be used to better constrain the density of the enclosed central dark mass, because their radial distances are greater than the minimum radius of 0.015 pc measured from the proper motion velocity experiment by Ghez et al. (1998). However, if the radial velocities of the three stars identified as early-type (S0-1, S0-2, S0-16) could be measured with future higher signal-to-noise spectra, sensitive to the He I and Br γ absorption lines expected to be present in these stars, than their 3D velocities could constrain the central dark mass density down to radii < 0.0075 pc, and further establish the configuration of the central dark matter

distribution as a central supermassive black hole, as opposed to a cluster of stellar remnants, or other more exotic forms of dark matter.

Acknowledgments. AG thanks H. Roe, C. McCabe, D. Kaisler, and S. Gezari for giving presentations at the CfAO 2000 summer school. This work has been supported in part by the National Science Foundation Science and Technology Center for Adaptive Optics, managed by the University of California at Santa Cruz under cooperative agreement No. AST-9876783, and in part by the National Science Foundation grant No. AST-998837.

References

- Babu, G. J., & Feigelson, E. D. *Astrostatistics*. 1996 *Chapman & Hall*, London, UK
- Genzel, R., Eckart, A., Ott, T., & Eisenhauer, F. 1997, *MNRAS*, 291, 219
- Genzel, R. Pichon, C., Eckart, A., Gerhard, O. E., & Ott, T. 2000, *MNRAS*, 317, 348
- Ghez, A.M., Neugebauer, G., and Matthews, K. 1993, *AJ*, 106, 2005
- Ghez, A.M., Klein, B.C., Morris, M., & Becklin, E.E. 1998, *ApJ*, 509, 678
- Ghez, A.M., Morris, M., Becklin, E.E., Tanner, A., & Kremenek, T. 2000, *Nature*, 407, 349
- Gibbard, S. G., Macintosh, B., Gavel, D., Max, C. E., de Pater, I., Ghez, A. M., Young, E. F., McKay, C. P. 1999, *Icarus*, 139, 189
- Hanson, M.M., Conti, P.S., & Rieke, M.J. 1996, *ApJS*, 107, 281
- Kleinmann, S.G., & Hall, D.N.B 1986, *ApJS*, 62, 501
- Koresko, C. D. 1998, *ApJ*, 507, 145L
- Koresko, C. D, Blake, G. A., Brown, M. E., Sargent, A. I., Koerner, D. W. 1999, *ApJ*, 525, 49L
- McLean, I.S. 1998, *Proc. SPIE*, 3354, 566
- Morris, M. 1993, *ApJ*, 408, 496
- Reid, M.J. 1993, *ARA&A*, 31, 345
- Wizinowich, P. et al. 2000, *Proc. SPIE*, 4007, 2